Chapter 3

SIMULATION OF DIELECTRIC FLUID AT IEG

3.1. INTRODUCTION

The study of the behavior of fluids in μchannel is generally referred as microfluidics. In microfluidics, the fluids are directed, mixed, separated or manipulated to perform desired task. Though this is similar to the science of fluidics, still the microscale behavior is largely different as compared at the macroscale. For the present study of μED-milling process, the flow of dielectric fluid along the IEG closely resembles the microfluidic theory. During machining, dielectric flows through the IEG continuously to establish spark, cool the ejected metal and removal of debris from the sparking zone. The flow of dielectric is very essential for the process to ensure regular discharge and uninterrupted material removal. This is a unique aspect of the μED-milling which is not generally required for conventional EDM process. Hence, understanding the behavior of dielectric flow along the IEG is critical for the machining performance of the process. The flow of dielectric is achieved by various methods such as tool rotation, tool vibration, tool jump or simply by injection of fluid through nozzle either externally or internally. Among the above listed methods, tool rotation is considered to be a suitable option for a μchannel of 500 μm with an IEG of 50 μm. The tool rotation not only enhances the fluid flow but also avoids deflection of tool due to shock waves. Additional drag is created on the dielectric by the injection of fresh fluid through the nozzle located at the inlet of μchannel. This chapter presents the microfluidic study along the IEG of μED-milling process through CFD simulation to understand the influence of parameters such as tool rotation speed, gap width (IEG), nozzle inlet velocity, and tool diameter on the average dielectric velocity and flow patterns. The study will provide useful insight to the complex phenomenon of μED-milling at the IEG.

3.2. SIMULATION PARAMETERS

The list of parameters considered for simulation is given in Table 3.1. As discussed earlier, kerosene is found to provide best performance and hence selected for simulation. The properties of kerosene necessary for simulation are viscosity, density, specific heat and thermal conductivity, whose values are listed in Table 3.1. These values are kept constant throughout the simulation. In μED-milling process, low value of viscosity is very essential property of dielectric to enable a thin layer to be dragged into the IEG as small as 50 μm. The primary drag force to the dielectric fluid is created by tool rotation. A minimum rotation speed of 100 rpm is required to initiate the discharge and avoid tool deflection by shock wave. Higher rotation speed can enhance the flushing of debris particles [83], but a value above 800 rpm is not found to affect MRR [84]. Therefore, three different tool rotation speeds such as 100, 500, and 800 rpm within the range are considered for simulation. The next parameter selected for simulation is IEG size which varies based on the energy applied in μED-milling process. The value of energy usually considered for the process varies between 50 to 2000 μJ. When the energy changes, the potential difference applied between the tool and workpiece is subjected to change which affects the IEG size. At low energy of 50 μJ, the IEG size is formed to be 10 μm and at high energy of 2000 μJ it is nearly 50 μm. The IEG size will affect the flow of dielectric and hence three values viz. 30, 40 and 50 μm are considered for simulation.

In addition to tool rotation, the nozzle inlet velocity will also provide sufficient drag force to the dielectric. The effect of nozzle injection (or inlet) velocity on the dielectric flow is also studied in simulation. A longer range of values from 0.001 cm/s to 100 cm/s is considered since such study is not found in literature and it affects both the responses namely, dielectric velocity at IEG and the pattern of fluid flow. The diameter of tool is another parameter which contributes to dielectric flow. The increase in the diameter of the tool increases the centrifugal force on the dielectric. Three different tool diameters viz. 300, 400 and 500 μm are considered for simulation as it is commonly used in μED-milling process.

Table 3.1 Input Parameters

Input Variables	Values
Dielectric fluid (Kerosene)	Kerosene (υ = 0.0116 cm^2/s, ρ = 860 kg/m^3, C_p = 2100 J/kg^{o}C, k = 0.14 W/mk
Tool rotation speed (rpm)	100, 500, 800
IEG size (μm)	30, 40, 50
Nozzle inlet velocity (cm/s)	0.001, 0.01, 0.1, 1, 10, 50, 100
Tool diameter (μm)	300, 400, 500

3.3. ANALYSIS POINTS

The dielectric fluid flow in IEG is simulated using a model of μchannel as discussed in Chapter 2 and the schematic diagram of the same is shown in Figure 3.1. For observation of simulated results, selected positions are considered across the IEG between the tool and workpiece. These positions are represented as I, II and III across the IEG as seen in Figure 3.1 such that the position I indicate near to workpiece, position II at the center and position III near to tool. At each position, three points are considered to measure the values of dielectric velocity and an average of these values is reported. The positions in Figure 3.1 also show that they are located at the front end of the tool and apparently the area behind the tool is referred as back end of the tool where the formation of vortex is observed (will be explained later in the discussion). This region at the back end of the tool is important to study the fluid flow pattern and the vortex behavior.

3.4. GENERAL FLOW PATTERN

In a two-dimensional steady flow, the streamlines are the line representing a free surface within the fixed boundary. In the absence of any object, the flow is laminar and the streamlines follow the regular path but it gets disturbed by the presence of external object. For example, if an external object is considered as a circular cylinder and is placed perpendicular to the flow direction then the cross flow creates complex flow pattern as

visible in Figure 3.2 (a). As noticed in the figure, when the fluid strikes the cylinder some streamlines are deflected and the one which is at the center of the flow will create a stagnation point. A stagnation point is a point in a flow-field where the velocity of the fluid is zero and the pressure is maximum. The stagnation point exists at the surface in the flow-field, where the fluid is brought to rest by the object. At low inflow velocity, the two streams of fluid encircle the cylinder will meet at the rear end on the cylinder but when the velocity is high it fails to meet at the rear end and causes low pressure region called wake. Hence when the inflow velocity is high, the pressure difference on the two sides of the cylinder will produce a net force on the cylinder in the direction of the flow. When the fluid is moving over the rotating cylinder some fluid is dragged by the cylinder which causes the stagnation points to shift down from the center as shown in Figure 3.2 (b). Now the flow is unsymmetrical about the horizontal plane (or center line) and the pressure on the top is less than the pressure at the bottom. This pressure difference exerts a force on the cylinder normal to the flow direction contradictory to the stationary cylinder condition. This phenomenon is known as the Magnus effect and it is commonly observed in fluid flow over rotating object [85].

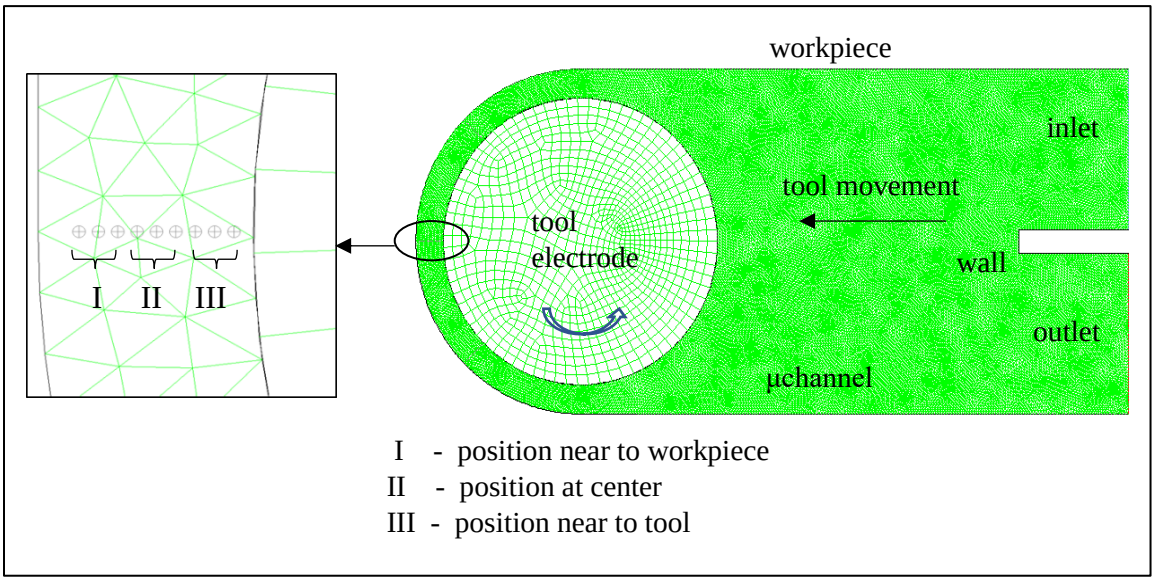

Figure 3.1 Schematic diagram representing the analysis points for model study

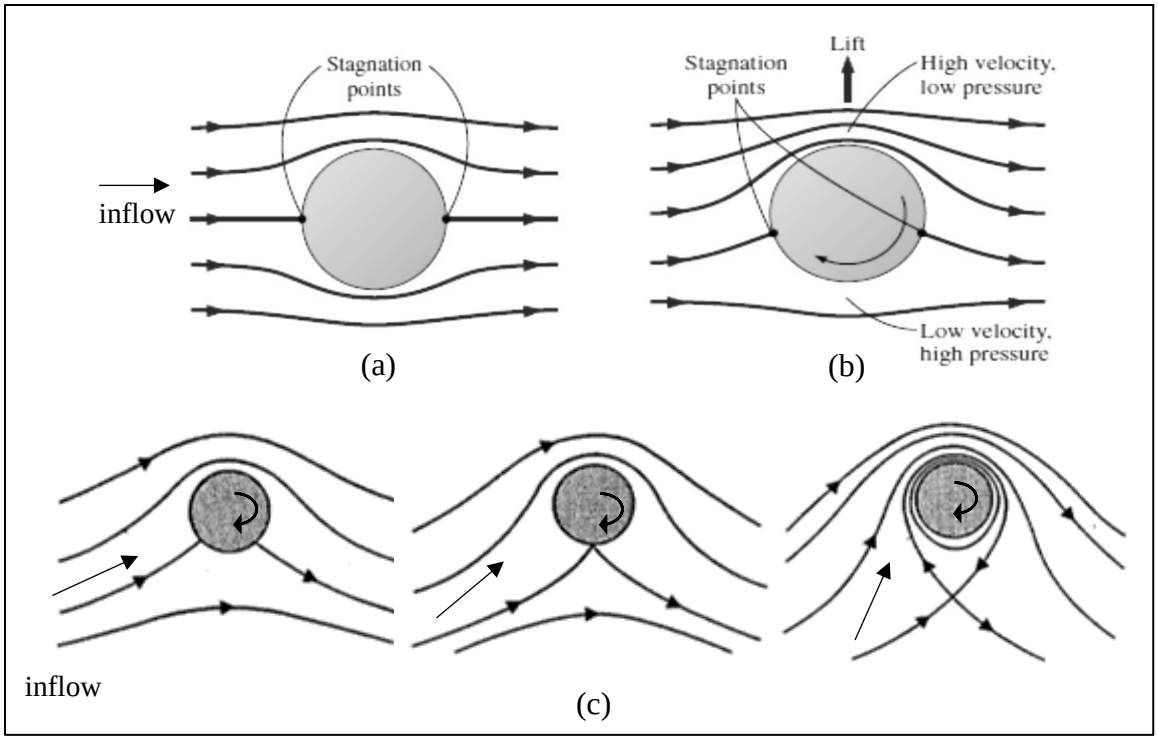

Figure 3.2 Schematic diagram showing (a) flow over stationary cylinder, (b) Magnus effect, and (c) flow over rotating cylinder with different inflow angle [85]

In µED-milling process, the flow of dielectric fluid from the nozzle inlet over the rotating tool can be considered similar to the situation of fluid flow over a rotating cylinder. The Magnus effect can move the tool perpendicular to its axis towards the workpiece causing instability. However, the servo mechanism of µED-milling process ensures constant gap between the tool and workpiece neglecting the Magnus effect. Therefore, for this simulation study, the Magnus effect is ignored and the tool position is considered unaffected by the dielectric flow. The fluid flow behavior also changes when the flow over the rotating cylinder approaches from different angles. Figure 3.2 (c) shows flow pattern for three different angles of approaches. When the angle of approach is small, two stagnation points are observed on the opposite sides of the cylinder similar to above discussion. However, when the angle increases to intermediate value, the stagnation point moves closer to each other and get merged. Further increase in the angle of approach (high value), moves the stagnation point away from the cylinder. This is similar to the simulation

model under consideration where the fluid flows with a large angle of approach and the stagnation point is observed away from the tool.

The schematic diagram showing different flow parameters in the simulation model is shown in Figure 3.3. The two-dimensional flow around a rotating circular cylinder near a plane wall depends mainly on four parameters: the Reynolds number, the boundary layer thickness on the plane wall, the rotation rate of the cylinder, and the gap between the cylinder and plane wall. The effect of turbulence due to vortex flow and the boundary layer thickness on the plane wall is considered in the turbulence model ($k - \varepsilon$) selected for simulation. The rotational rate (γ) is given by

$$\gamma = \frac{\omega\, a}{U} \tag{3.1}$$

where ω is the angular velocity of the rotating cylinder, a is the radius of cylinder, and U is the inflow velocity. The rotational rate is the important parameter which is the tangential velocity ($\omega\, a$) normalized by the inflow velocity. It is a unitless number and higher value of it represents that the flow is dominated by the rotation of the cylinder. The fluid in a region near the cylinder is dragged by the cylinder due to viscous force. When the rotational rate is high, the region affected by the viscous force is also greater. In addition, if a plane wall is present in the flow the symmetry of the flow is completely altered and the flow-field now depends on the rotational rate and the normalized gap. The normalized gap (h) is given by

$$h = \frac{H}{D} \tag{3.2}$$

where H is the gap between cylinder and plane wall, and D is the cylinder diameter. The presence of a plane wall in the flow breaks the flow symmetry and leads to complex flow patterns. The discussion of the flow pattern in the μchannel which is affected by tool speed, gap size, inlet velocity, and the tool diameter is presented in the subsequent section. The schematic diagram showing the flow-field observed in the μchannel is represented in Figure 3.4. The fluid flow in the IEG is uniform and follows the definite path. The formation of vortex at the back of tool changes the fluid flow direction and this creates a

region on either side of the tool where the velocity of fluid is less. The flow-field in the μchannel basically consists of vortices, stagnation point, and flow separation.

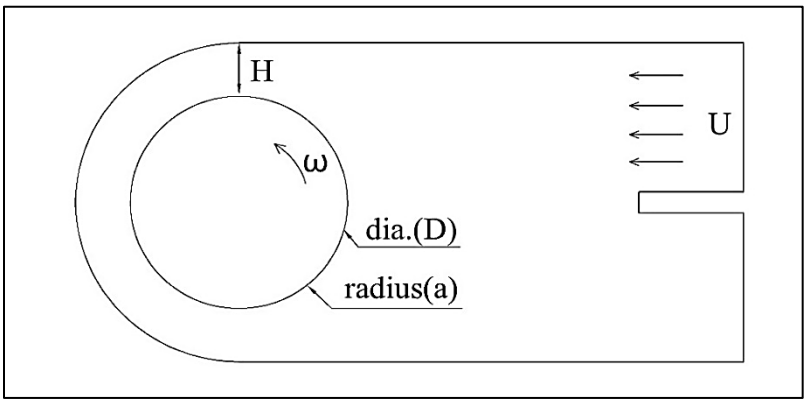

Figure 3.3 Schematic diagram showing flow parameters in the μchannel

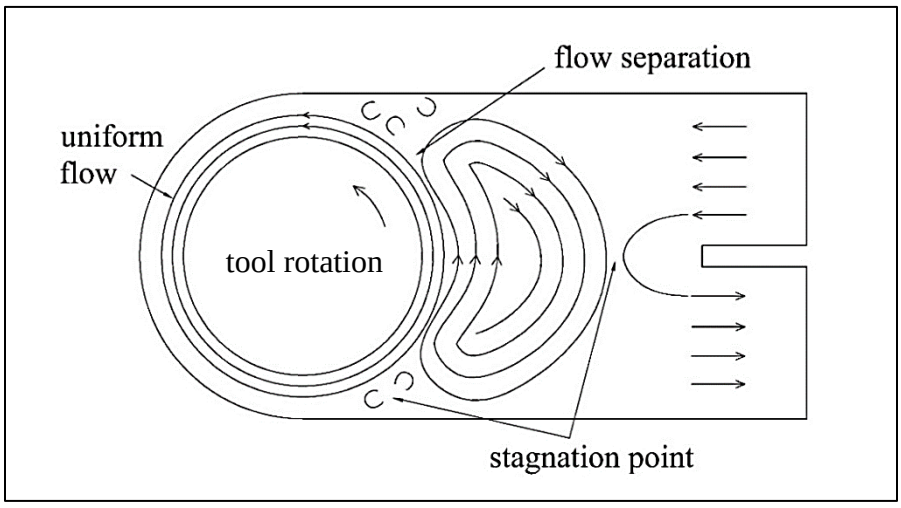

Figure 3.4 Schematic diagram showing flow-field in the μchannel

3.5. INFLUENCE OF PARAMETERS ON DIELECTRIC FLUID FLOW

3.5.1. Effect of tool rotation speed

The average dielectric velocity at the IEG is greatly affected by the tool rotation speed. The average dielectric velocity at the IEG when the gap width is 50 μm and the nozzle inlet velocity is 0.01 cm/s is shown in Figure 3.5. With the increase in the tool speed,

the average dielectric velocity in the gap increases. The average dielectric velocity is minimum near the workpiece surface and it is maximum near the tool. The reason is that the fluid layer in contact with the tool experiences a centrifugal force due to tool rotation. While near the workpiece the dielectric is brought to rest as it acts as a barrier to the free flow of the dielectric. At the center, the value of average dielectric velocity lies in between the two. The velocity along the circumference of the tool remains constant and it varies radially towards the workpiece surface. As the tool rotation is the important parameter the effect of other input parameters is analyzed at different tool speed.

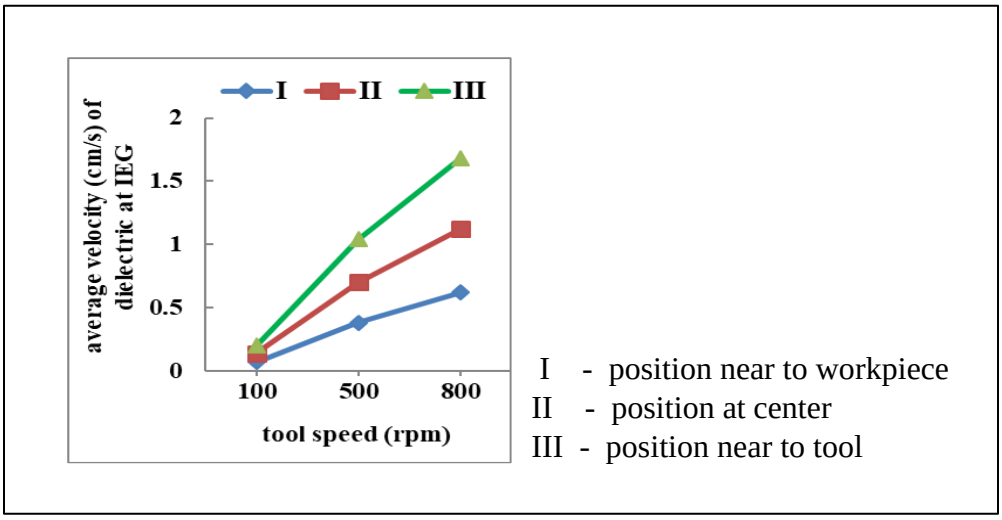

Figure 3.5 Effect of tool rotation speed on the average dielectric velocity at IEG

Figure 3.6 shows the velocity vector plots for the different cases such as stationary tool with wall, rotating tool without wall, and the direction of tool rotation. In all the cases, the inlet and outlet sections are present on either side of the wall. The dielectric fluid is supplied through inlet with a velocity of 0.01 cm/s. In the first case, the tool is held stationary and the dielectric is supplied through the inlet as shown in Figure 3.6 (a). The large amount of fluid enters the μchannel and backflows from the outlet section. As the tool is stationary and the maximum portion of the fluid flows back, the velocity at the IEG does not increase. The dielectric fluid near the tool is stagnant and not moving. In the second case, the tool is rotated in counter-clockwise direction and the unit thickness of wall

is considered to differentiate inlet and outlet section as represented in Figure 3.6 (b). The tool rotation drags the dielectric fluid in the gap and the force is exerted on the fluid increasing its velocity in the gap. The presence of spiral and center point shows that a vortex is present. The vortex is observed at the back of the tool. In the absence of the wall some fluid leaves through the outlet and it does not affect the flow pattern near the tool. This shows that the assumption made during the problem description regarding imaginary wall is true. In the third case, tool is rotated in different directions in the presence of wall to study the fluid pattern as shown in Figure 3.6 (c) and (d). When the tool rotates in counter-clockwise direction, the vortex flow is in clockwise direction and when the tool rotates in clockwise direction, the vortex flow is in counter-clockwise direction. The center of the vortex is the finite region around which the fluid rotates. The velocity at the center of the vortex is low and it increases at the outermost layer. In all the cases, it is seen that when the tool is rotating the velocity in the IEG is large which shows that the tool rotation is a major driving force to increase the dielectric velocity in the gap.

The contour plots of static pressure for gap size of 50 μm and the tool rotation at 500 rpm is shown in Figure 3.7. The gap inlet represents the region where the fluid enters the IEG and the gap outlet represents the region where the fluid leaves the IEG. The pressure varies along the gap between the tool and workpiece and the large variation is observed at the gap inlet and the gap outlet. The flow is accelerated near the gap outlet and hence the pressure is low, whereas it is decelerated at the gap inlet increasing the pressure. The variation in pressure is observed for all the cases discussed in the previous section. According to the Bernoulli's equation static pressure is high when the velocity is zero and it is referred as stagnation pressure, this pressure is equal to the total pressure in case of incompressible flows. When the tool rotation direction is clockwise the pressure affected region gets altered due to change in the position of gap inlet and outlet as shown in Figure 3.7.

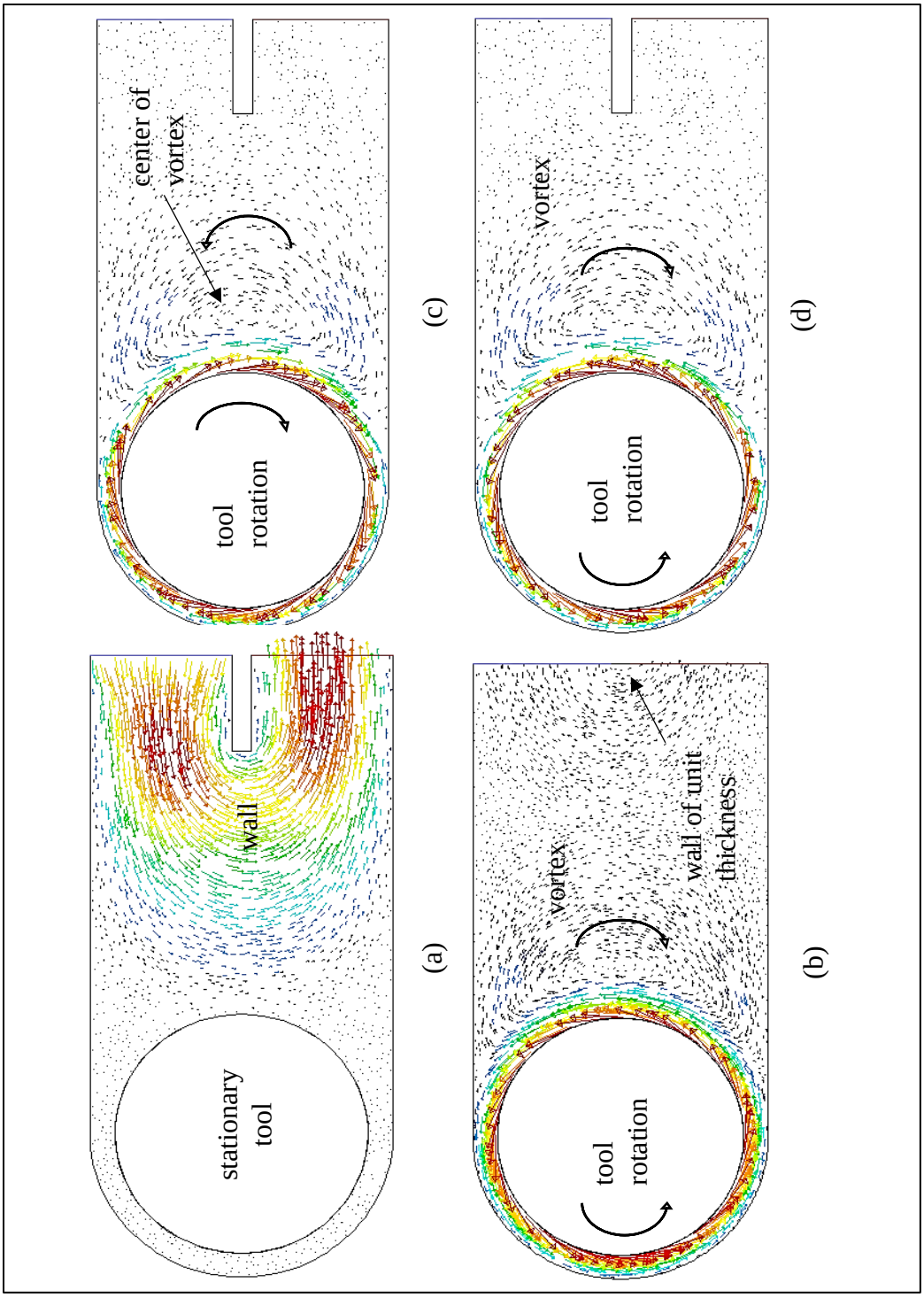

Figure 3.6 Velocity vector showing (a) stationary tool, (b) rotating tool with a wall of unit thickness, (c) clockwise rotation, and (d) counter-clockwise rotation considering wall

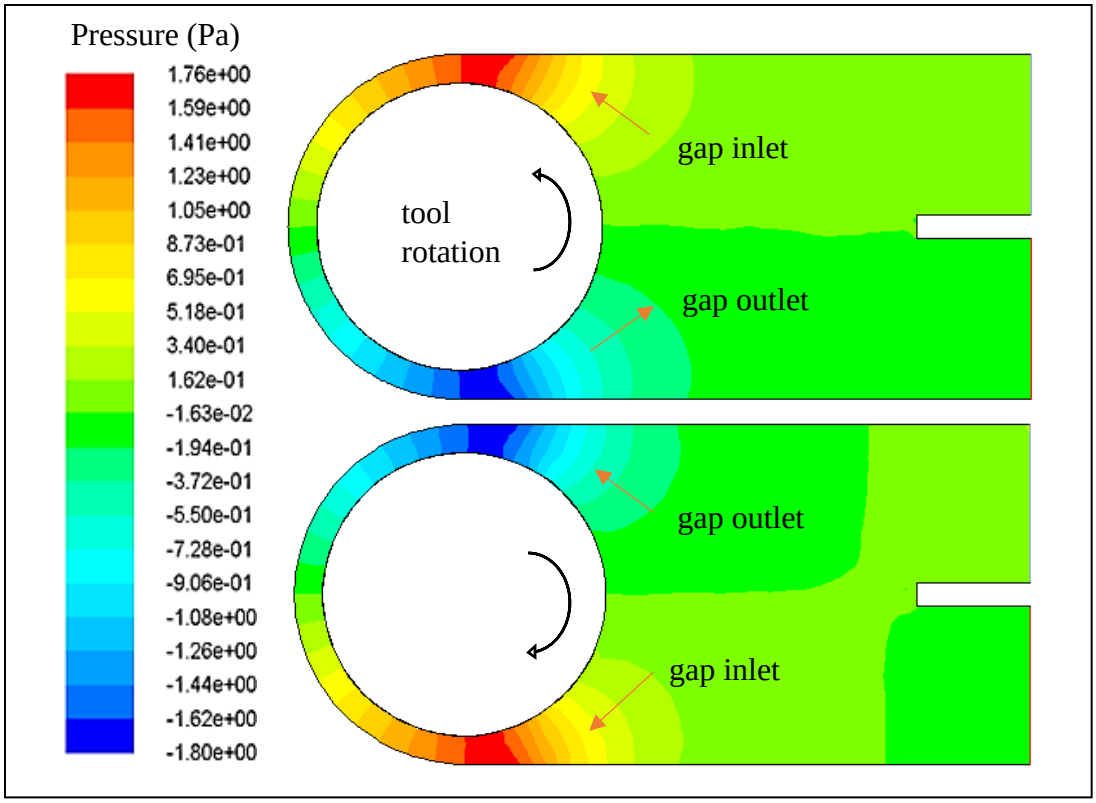

Figure 3.7 Static pressure (Pa) contour plots in the µchannel

3.5.2. Effect of interelectrode gap

The effect of gap size on the dielectric velocity at the IEG is studied for three different tool rotation speeds as discussed earlier. The gap is varied in two ways: in the first case the tool diameter is varied and the width of µchannel is kept constant and in the second case the width of µchannel is varied and the tool diameter is kept constant. The dielectric is supplied with a constant nozzle inlet velocity of 0.01 cm/s. In the first case, the sizes of gap considered for simulation are 30, 40 and 50 µm with the corresponding tool diameters of 540, 520 and 500 µm respectively. The µchannel width is kept constant at 600 µm. Figure 3.8 shows the effect of IEG on dielectric velocity when the µchannel width is kept constant and tool diameter is varied to change the gap. It shows that as the gap size increases, the average dielectric velocity in the gap decreases for position II and position III and this drop is maximum when the velocity is measured near the tool. At position I,

the average dielectric velocity remains constant for all conditions. As tool speed increases, the average velocity across the gap increases as expected. This implies that when the gap is small, the flushing is better if the debris appears close to the tool because of the higher dielectric velocity at that position. However, for a given position of IEG, the velocity does not seem to be affected by the variation in the gap. Thus, the fluctuation in voltage or irregularity in surface peaks which causes small variation in the gap does not affect the dielectric movement along the IEG. In the µED-milling process where the energy is less and the gap is small, this observation of an increase in dielectric velocity will ensure continuous discharge and subsequent material removal which is needed for the process. The aid of tool rotation and the increase of dielectric velocity at small gap will provide effective flushing for the µED-milling process.

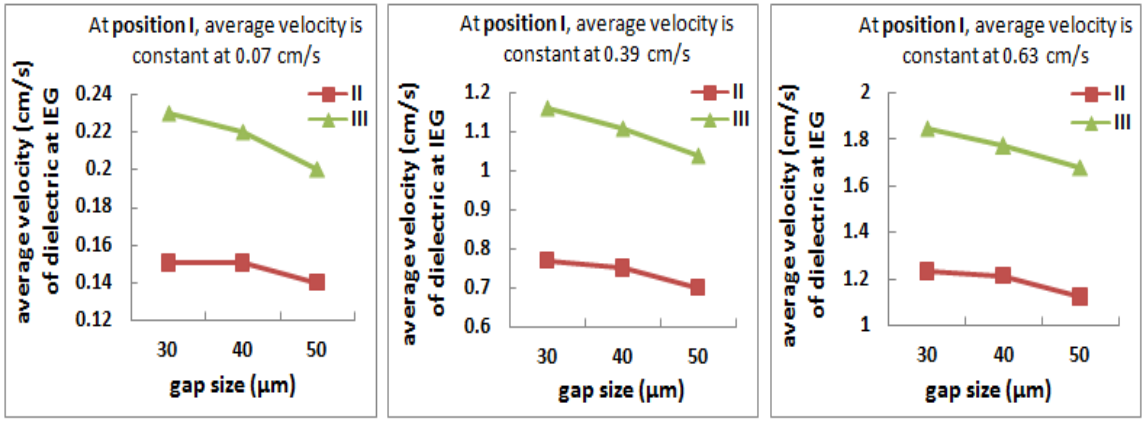

(a) (b) (c)

Figure 3.8 Effect of gap size on the average dielectric velocity at IEG for electrode speed of (a) 100 (b) 500 and (c) 800 rpm. The µchannel width is kept constant and electrode diameter is varied to change the gap

In the second case, the tool diameter is kept constant at 500 µm and µchannel width is varied to 560, 580 and 600 µm to change the gap width. Figure 3.9 shows the effect of gap width on dielectric velocity at IEG at tool speed of 100 rpm. The average dielectric velocity remains constant for various tool speeds and hence the values at 100 rpm are presented in figure. This result implies that when the diameter of the tool is constant and the gap size changes due to input energy the dielectric velocity will remain constant. In

addition, an increase in the diameter of the electrode will increase the centrifugal force on the fluid increasing its velocity in the gap.

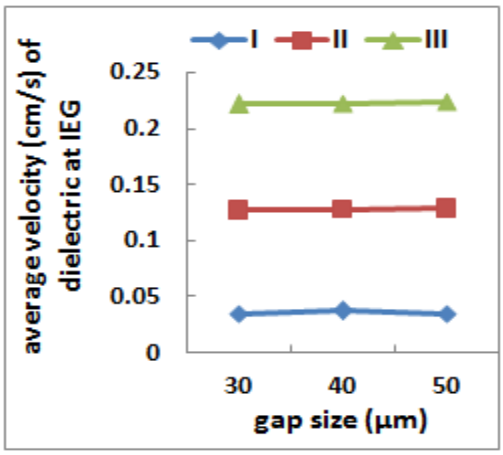

Figure 3.9 Effect of gap size on the average dielectric velocity at IEG for electrode speed of 100 rpm. Electrode diameter is kept constant and µchannel width is varied to change the gap

3.5.3. Effect of inlet velocity of the dielectric fluid

The inlet velocity refers to the jet velocity of the dielectric near the entrance of the µchannel. The velocity at the inlet is varied from 0.001 to 100 cm/s for the initial study. It is observed that when the nozzle inlet velocity is varied between 0.001 to 10 cm/s, the average dielectric velocity at IEG remains constant which is given in Table 3.2. At lower nozzle inlet velocity, the effect of tool rotation speed is dominant and hence velocity at the IEG remains constant irrespective of the change in nozzle inlet velocity. However, when the velocity increases above 10 cm/s, there is a significant rise in the velocity of the dielectric at the IEG as shown in Figure 3.10. This increase in dielectric velocity at IEG is due to the nozzling effect near the gap inlet. The effect is further enhanced by an increase in tool rotation speed which clearly shows that two effects are independent of each other. This behavior of increase in dielectric velocity at IEG happens for all the positions, and hence irrelevant of where the debris appears in the gap, flushing will be efficient.

Table 3.2 Average dielectric velocity at IEG (cm/s)

Tool speed (rpm)	Position at IEG		
	I	II	III
100	0.06	0.11	0.16
500	0.31	0.57	0.81
800	0.49	0.92	1.3

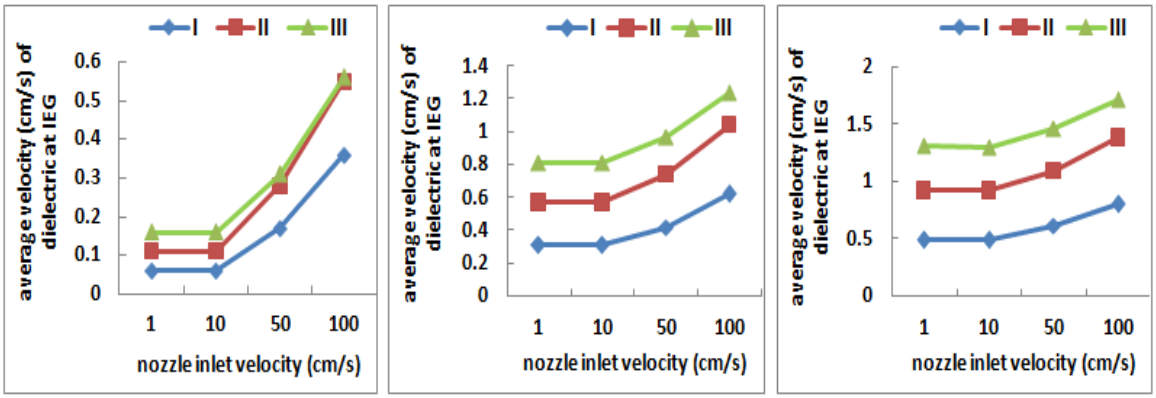

(a) (b) (c)

Figure 3.10 Effect of nozzle inlet velocity on the average dielectric velocity at IEG for electrode speed of (a) 100 (b) 500 and (c) 800 rpm

The velocity at the IEG remains constant for the lower nozzle inlet velocity but it affects the fluid flow pattern as shown in Figure 3.11. At lower inlet velocity of 0.001 cm/s, the vortex is created at the back of the tool as shown in Figure 3.11 (a) which acts as a secondary stirrer. The vortex flow occupies the whole width of the μchannel. The center of the vortex has zero velocity and its position is constant as seen in the figure. The increase in tool speed increases the velocity in the IEG, but the considerable change in the vortex flow pattern is not observed. With the increase in the inlet velocity to 0.01 cm/s and a tool speed of 100 and 500 rpm, the shape of the vortex remains same. However, when the tool speed is increased to 800 rpm, the size of vortex decreases at one end and it looks like conical shape as shown in Figure 3.11 (b). The incoming fluid does not enter the IEG easily due to which it suppresses the vortex and makes it conical at the end and hence the

stagnation point is observed at that point. Further increase in the inlet velocity to 0.1 cm/s and at lower tool speed of 100 rpm, the vortex breakdowns and most of the fluid moves back from the outlet section as shown in Figure 3.11 (c). Although with the increase in the tool speed, the vortex is observed with smaller size and elongated at one end. This shows that the formation of vortex depends on the tool rotation speed and the inlet velocity. At this stage, the stagnation points are visible near the wall with a small shift which is caused due to tool rotation. The vortex is not observed when the inlet velocity is increased above 1 cm/s and all the fluid moves back from the outlet section as shown in Figure 3.11 (d). Hence only increasing the jet velocity is not effective in increasing the velocity at the IEG but the tool speed can be effectively used to drag the dielectric at the IEG.

3.5.4. Effect of change in dimension of tool

In this study, the dimension of the μchannel and tool is changed without changing the gap width. The size of the μchannel width considered is 400, 500 and 600 μm with a corresponding tool diameter of 300, 400 and 500 μm respectively. This can definitely happen in real time while machining different μchannels of various size with same energy conditions. The gap width of 50 μm is kept constant for all the combinations. The variation in the vortex size is observed with the change in the dimension of the μchannel. At lower tool diameter, the width of the vortex occupies the channel width and with the higher tool diameter, the vortex with smaller size is observed and it is elongated at the end. This is due to the combined effect of an increase in velocity due to tool diameter and the inlet velocity which compresses the vortex to make it conical at the end. Figure 3.12 shows the average velocity for different size combinations of tool and μchannel width. As expected, when tool rotation speed increases, the corresponding dielectric velocity at IEG increases, and when the tool diameter decreases the average dielectric velocity decreases. So higher the tool diameter with a constant gap, greater the centrifugal force, greater the velocity at the IEG and better is the flushing as explained earlier.

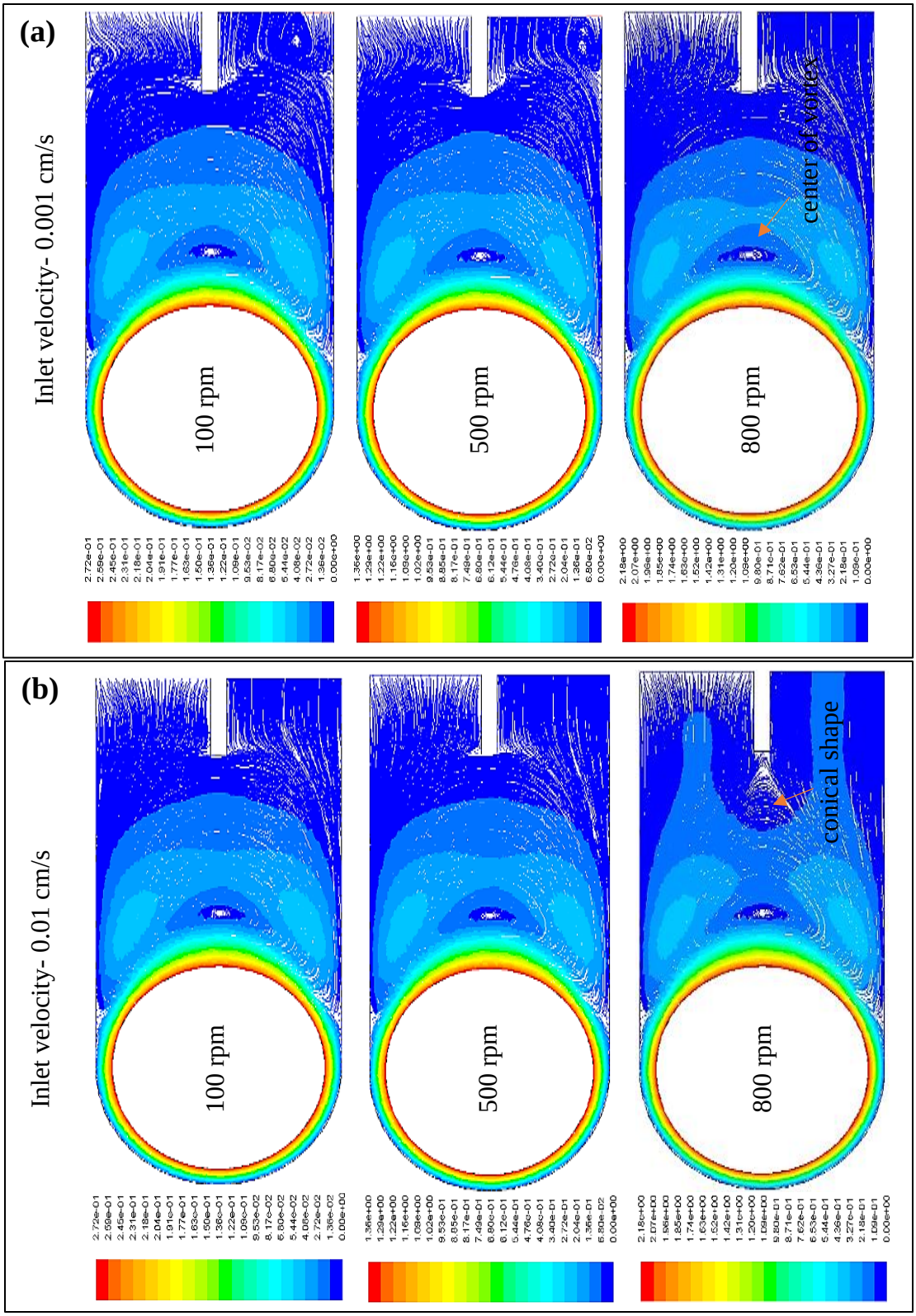
(a)
Inlet velocity- 0.001 cm/s
100 rpm
500 rpm
800 rpm
center of vortex
(b)
Inlet velocity- 0.01 cm/s
100 rpm
500 rpm
800 rpm
conical shape

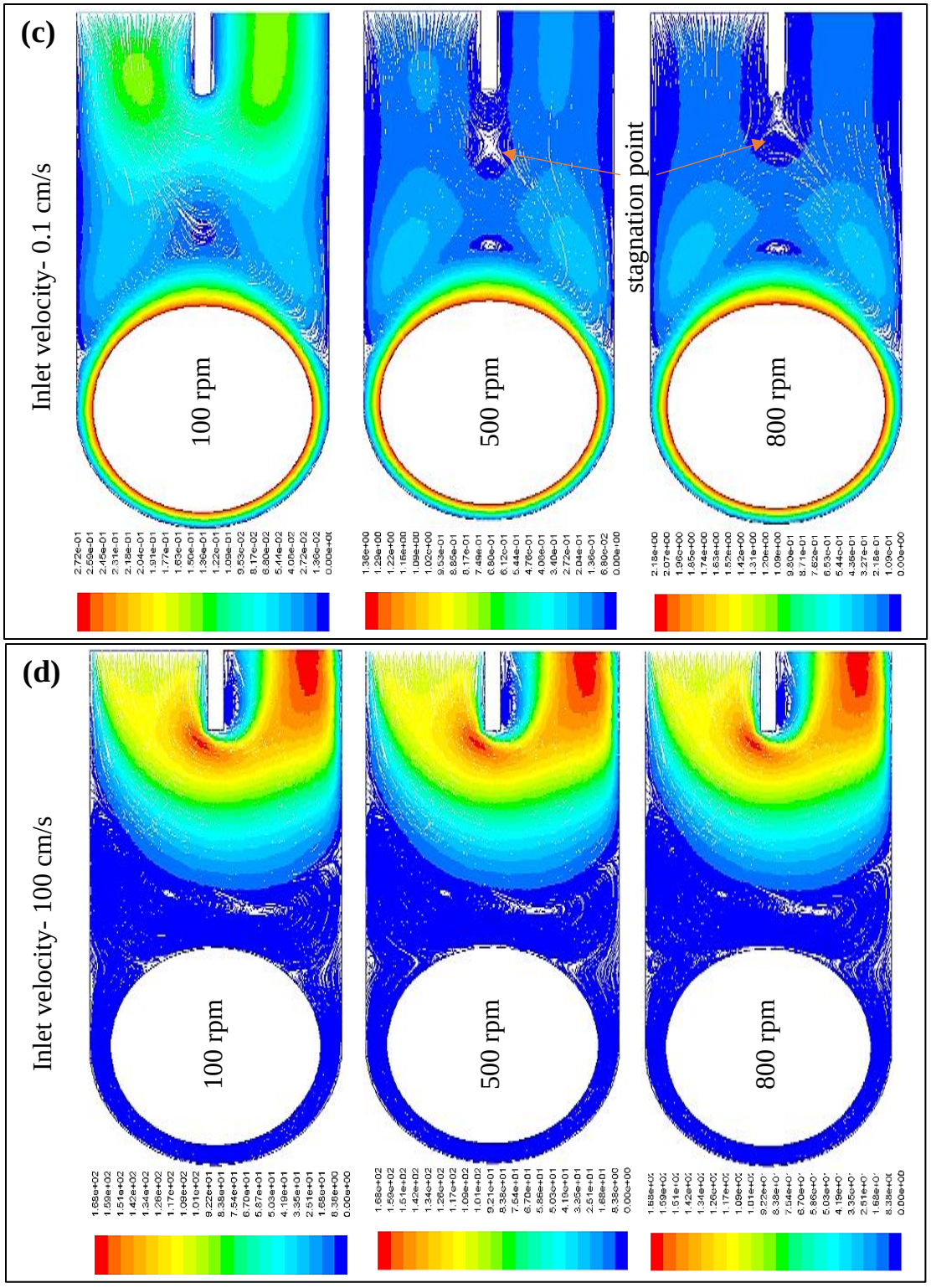

Figure 3.11 Velocity path lines of the dielectric at various nozzle inlet velocity

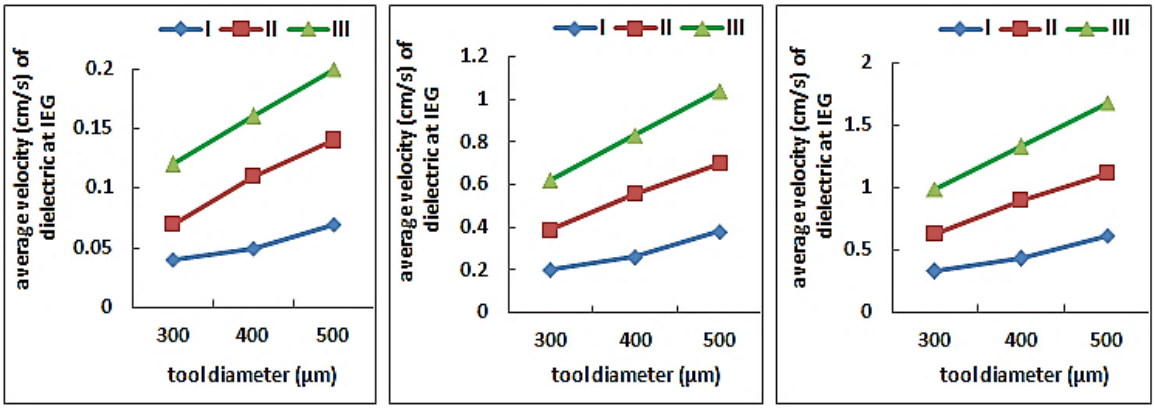

(a) (b) (c)

Figure 3.12 Effect of tool diameter on the average dielectric velocity at IEG for tool speed of (a) 100 (b) 500 and (c) 800 rpm

3.6. SUMMARY

The dielectric flow velocity at the IEG determines the debris flushing from the gap. The flow pattern decides the direction of the debris flow in the gap. The size and shape of the debris and surface texture formed depend on fluid velocity in the gap. The simulation results showed that as the gap size decreases, the average velocity of the fluid in the gap increases. In µED-milling, as the tool is rotating at high speed, the fluid in contact with the tool will rotate at high speed and the speed reduce across the gap towards the stationary workpiece. The average dielectric velocity in the gap is affected by the change in nozzle inlet velocity, also there is a change in fluid pattern which create vortices. Vortex created at the back of the tool act as a secondary stirrer in the process. They supply fresh dielectric in the gap and remove debris particles from the gap. The fluid flow in the µchannel basically consists of vortices, stagnation points, and separation points.